Fizika Nizkikh Temperatur, 1997, v. 23, No 7, p. 721–726

Dynamic susceptibility of spin-1/2 Ising chain in transverse field

O. Derzhko and T. Krokhmalskii

Institute for Condensed Matter Physics, 1 Svientsitskii St., L'viv-11, 290011, Ukraine
E-mail: derzhko@icmp.lviv.ua
krokhm@icmp.lviv.ua

Submitted December 5, 1996

Dynamic susceptibility of the one-dimensional spin-1/2 transverse Ising model is obtained by using the numerical approach suggested earlier [*Ferroelectrics* **153**, 55 (1996)]. The dependence of the susceptibility frequency shapes on the value of the transverse field at various temperatures is discussed. The way in which the frequency shape rebuilds as the transverse field increases is illustrated.

PACS: **75.10.–b**

The one-dimensional spin-1/2 Ising model in a transverse field is an important subject of theoretical studies not only because of its usefulness in solid state physics, but also because many of its statistical mechanics properties can be examined exactly [1–3]. However, since the early 1970s it was known that calculation of some time-dependent spin correlation functions for this model encounter great difficulties and in spite of many papers dealing with this problem [4–7] (see also recent papers [8,9] dealing with such studies for the one-dimensional spin-1/2 XX model) the investigation of dynamic properties calls for more efforts. In the present paper our goal is to provide a fresh view on the analysis of spin dynamics. Specifically, we shall extend the earlier elaborated numerical approach for equilibrium statistical mechanics calculations for spin-1/2 XY chains [10,11] to the analysis of dynamic properties of transverse Ising model and we shall study, in particular, its dynamic susceptibility.

We consider spin-1/2 chain described by the Hamiltonian

$$H = \Omega \sum_{j=1}^{N} s_j^z + J \sum_{j=1}^{N-1} s_j^x \, s_{j+1}^x \,, \qquad (1)$$

where Ω is the transverse field at the site, and J is the interaction between neighboring sites. Two distinctive cases corresponding to different signs of intersite interaction will be considered, i.e., $J < 0$ (ferromagnetic coupling) and $J > 0$ (antiferromagnetic coupling). We are interested in the time-dependent, two-spin correlation functions $\langle s_j^{\alpha}(t) s_{j+n}^{\beta} \rangle$, where the angle brackets denote thermodynamic average $\langle\langle (\ldots) \rangle\rangle \equiv \mathrm{Tr}\, [\mathrm{e}^{-\beta H}(\ldots)] / \mathrm{Tr}\, \mathrm{e}^{-\beta H}$. The correlation function between the z-components was derived in Ref. 2. We shall restrict the analysis mainly to the correlation function between the x-components of two spins, noting that all other nonzero correlation functions can be found in principle by differentiation:

$$\langle s_j^x(t) s_{j+n}^y \rangle = -\langle s_j^y(t) s_{j+n}^x \rangle = \frac{1}{\Omega} \frac{d}{dt} \langle s_j^x(t) s_{j+n}^x \rangle \,,$$
$$\langle s_j^y(t) s_{j+n}^y \rangle = -\frac{1}{\Omega^2} \frac{d^2}{dt^2} \langle s_j^x(t) s_{j+n}^x \rangle \,. \qquad (2)$$

In order to evaluate the quantity of interest, one should rewrite the Hamiltonian (1) in terms of Fermi operators with the help of the Jordan-Wigner transformation and then diagonalize the bilinear fermion form. Basic results may be summarized as follows: The relations between spin operators and Fermi operators are

$$s_j^x = \frac{1}{2}\,\varphi_1^+\varphi_1^-\varphi_2^+\varphi_2^- \cdots \varphi_{j-1}^+\varphi_{j-1}^-\varphi_j^+ ,$$

$$s_j^y = \frac{1}{2i}\,\varphi_1^+\varphi_1^-\varphi_2^+\varphi_2^- \cdots \varphi_{j-1}^+\varphi_{j-1}^-\varphi_j^- , \qquad (3)$$

$$s_j^z = -\frac{1}{2}\,\varphi_j^+\varphi_j^- ,$$

where

$$\varphi_j^+ = \sum_{p=1}^{N} \Phi_{pj}\left(\eta_p^+ + \eta_p\right), \quad \varphi_j^- = \sum_{p=1}^{N} \Psi_{pj}\left(\eta_p^+ - \eta_p\right); \qquad (4)$$

the transformed Hamiltonian (1) has the form

$$H = \sum_{k=1}^{N} \Lambda_k \left(\eta_k^+\eta_k - \frac{1}{2}\right), \qquad (5)$$

$$\left\{\eta_q\ ,\ \eta_r^+\right\} = \delta_{qr}\ ,\ \ \left\{\eta_q\ ,\ \eta_r\right\} = \left\{\eta_q^+\ ,\ \eta_r^+\right\} = 0\ ;$$

Λ_p , Φ_{pj} , and Ψ_{pj} are determined from the equations

$$\sum_{j=1}^{N} \Psi_{pj}\,(A_{jn} + B_{jn}) = \Lambda_p \Phi_{pn} ,$$

$$\sum_{j=1}^{N} \Phi_{pj}\,(A_{jn} - B_{jn}) = \Lambda_p \Psi_{pn} ,$$

$$\sum_{j=1}^{N} \Phi_{qj}\,\Phi_{rj} = \sum_{j=1}^{N} \Psi_{qj}\,\Psi_{rj} = \delta_{qr} , \qquad (6)$$

$$\sum_{p=1}^{N} \Phi_{pi}\,\Phi_{pj} = \sum_{p=1}^{N} \Psi_{pi}\,\Psi_{pj} = \delta_{ij}$$

with

$$A_{ij} \equiv \Omega\delta_{ij} + \frac{J}{4}\,\delta_{j,i+1} + \frac{J}{4}\,\delta_{j,i-1} ,$$

$$B_{ij} \equiv \frac{J}{4}\,\delta_{j,i+1} - \frac{J}{4}\,\delta_{j,i-1} .$$

For further details see Refs. 1,10, and 11. In view of (3)–(5), the calculation of $\langle s_j^x(t)s_{j+n}^x\rangle$ reduces to exploiting of the Wick–Bloch–de Dominicis theorem and the result can be expressed compactly in the form of the Pfaffian of $2(2j+n-1)\times 2(2j+n-1)$ antisymmetric matrix constructed from elementary contractions

$$4\langle s_j^x(t)s_{j+n}^x\rangle = \langle\varphi_1^+(t)\varphi_1^-(t)\varphi_2^+(t)\varphi_2^-(t) \cdots \varphi_{j-1}^+(t)\varphi_{j-1}^-(t)\varphi_j^+(t)\varphi_1^+\varphi_1^-\varphi_2^+\varphi_2^- \cdots \varphi_{j-1}^+\varphi_{j-1}^-\varphi_j^+\varphi_j^-\varphi_{j+1}^+\varphi_{j+1}^- \cdots \varphi_{j+n-1}^+\varphi_{j+n-1}^-\varphi_{j+n}^+\rangle =$$

$$= \mathrm{Pf}\begin{pmatrix} 0 & \langle\varphi_1^+\varphi_1^-\rangle & \langle\varphi_1^+\varphi_2^+\rangle & \cdots & \langle\varphi_1^+(t)\varphi_{j+n}^+\rangle \\ -\langle\varphi_1^+\varphi_1^-\rangle & 0 & \langle\varphi_1^-\varphi_2^+\rangle & \cdots & \langle\varphi_1^-(t)\varphi_{j+n}^+\rangle \\ \vdots & \vdots & \vdots & \cdots & \vdots \\ -\langle\varphi_1^+(t)\varphi_{j+n}^+\rangle & -\langle\varphi_1^-(t)\varphi_{j+n}^+\rangle & -\langle\varphi_2^+(t)\varphi_{j+n}^+\rangle & \cdots & 0 \end{pmatrix}, \qquad (7)$$

where

$$\langle\varphi_j^+(t)\varphi_m^+\rangle = \sum_{p=1}^{N} \Phi_{pj}\,\Phi_{pm}\,\frac{\cosh\left[i\Lambda_p t - (\beta\Lambda_p/2)\right]}{\cosh\,(\beta\Lambda_p/2)} ,$$

$$\langle\varphi_j^+(t)\varphi_m^-\rangle = -\sum_{p=1}^{N} \Phi_{pj}\,\Psi_{pm}\,\frac{\sinh\left[i\Lambda_p t - (\beta\Lambda_p/2)\right]}{\cosh\,(\beta\Lambda_p/2)} ,$$

$$\langle\varphi_j^-(t)\varphi_m^+\rangle = \sum_{p=1}^{N} \Psi_{pj}\,\Phi_{pm}\,\frac{\sinh\left[i\Lambda_p t - (\beta\Lambda_p/2)\right]}{\cosh\,(\beta\Lambda_p/2)} , \qquad (8)$$

$$\langle\varphi_j^-(t)\varphi_m^-\rangle = -\sum_{p=1}^{N} \Psi_{pj}\,\Psi_{pm}\,\frac{\cosh\left[i\Lambda_p t - (\beta\Lambda_p/2)\right]}{\cosh\,(\beta\Lambda_p/2)} .$$

Equations (6)–(8) form the starting point for further numerical calculations. Considering a chain of $N = 280$ spins with $J = \pm 1$ and a certain value of the transverse field in the range $\Omega = 0.1$–5, we solved $N\times N$ standard problem (6) obtained in the result Λ_p , Φ_{pj} , Ψ_{pj} . Setting $j = 32$ and certain n in the range from 0 to 30, we then computed elementary contractions (8) involved in (7) for a given temperature in the range $\beta = 10$–0.1 and time t up to 120 and evaluated the Pfaffian numerically obtaining in the result the quantity of interest, i.e., the correlation between the x-components of spins at the sites j and $j + n$ taken at times t and $t = 0$, respectively. There are few practical limitations on this approach, i.e., finite chain size N, presence of boundaries $1 \le j, j+n \le N$, and finite time t. These effects lead to deviation from a time behavior inherent to an infinite chain, which is the case of interest

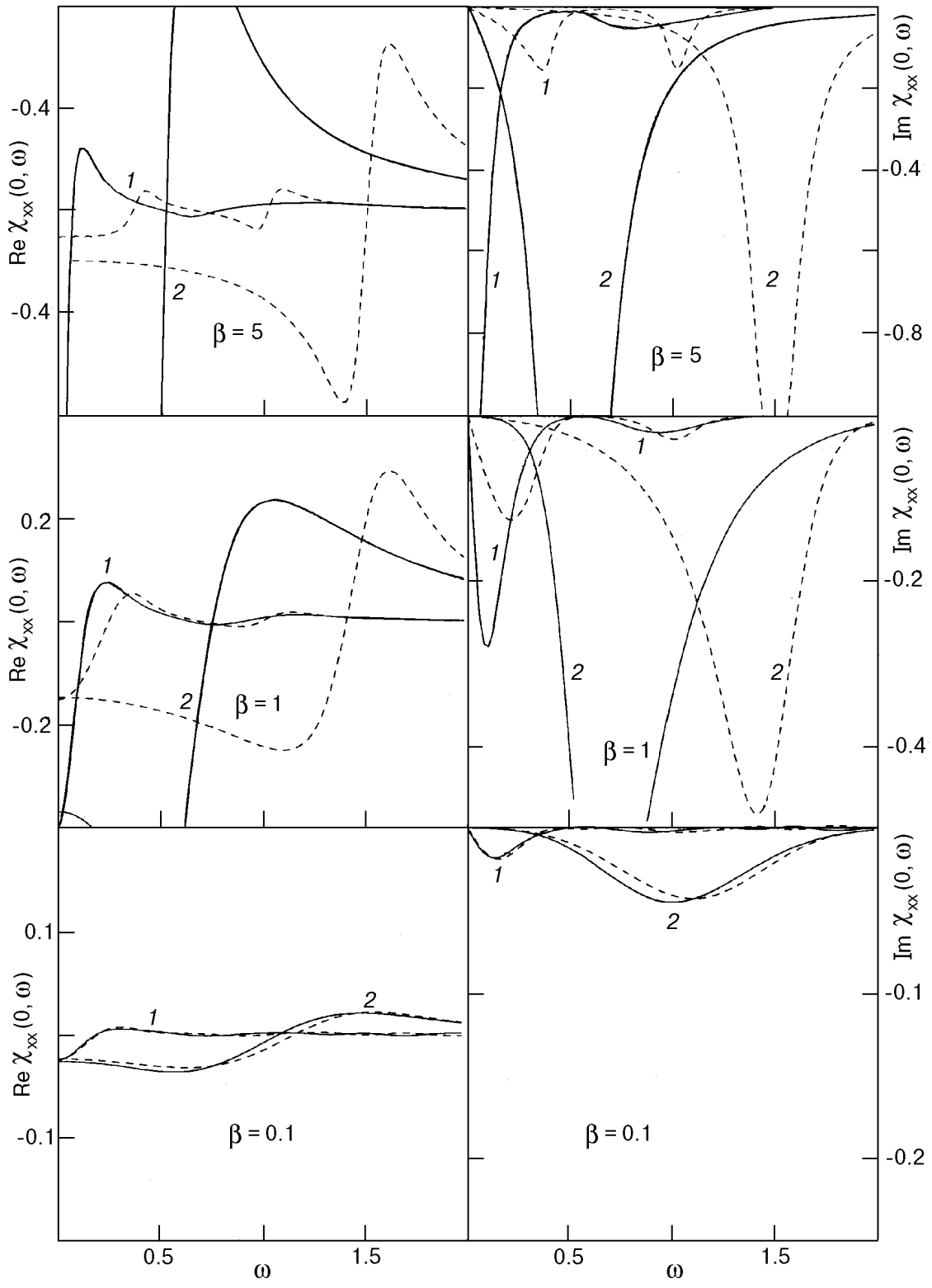

Fig. 1. $\chi_{xx}(0, \omega)$ versus ω at various temperatures. The solid lines represent data for ferromagnetic intersite coupling $J = -1$, the dashed lines denote data for antiferromagnetic intersite coupling $J = 1$; *1* corresponds to $\Omega = 0.2$; *2* corresponds to $\Omega = 1$.

in statistical mechanics. The value of this deviation depends on the values of the transverse field and the temperature. Nevertheless, since such effect is easy to recognize, one may derive in a wide range of parameters the results which are not subject to these influences, i.e., which refer to $N \to \infty$. The data produced in the calculations described above [as well as the results for $\chi_{xx}(\kappa, \omega)$ (9) obtained on

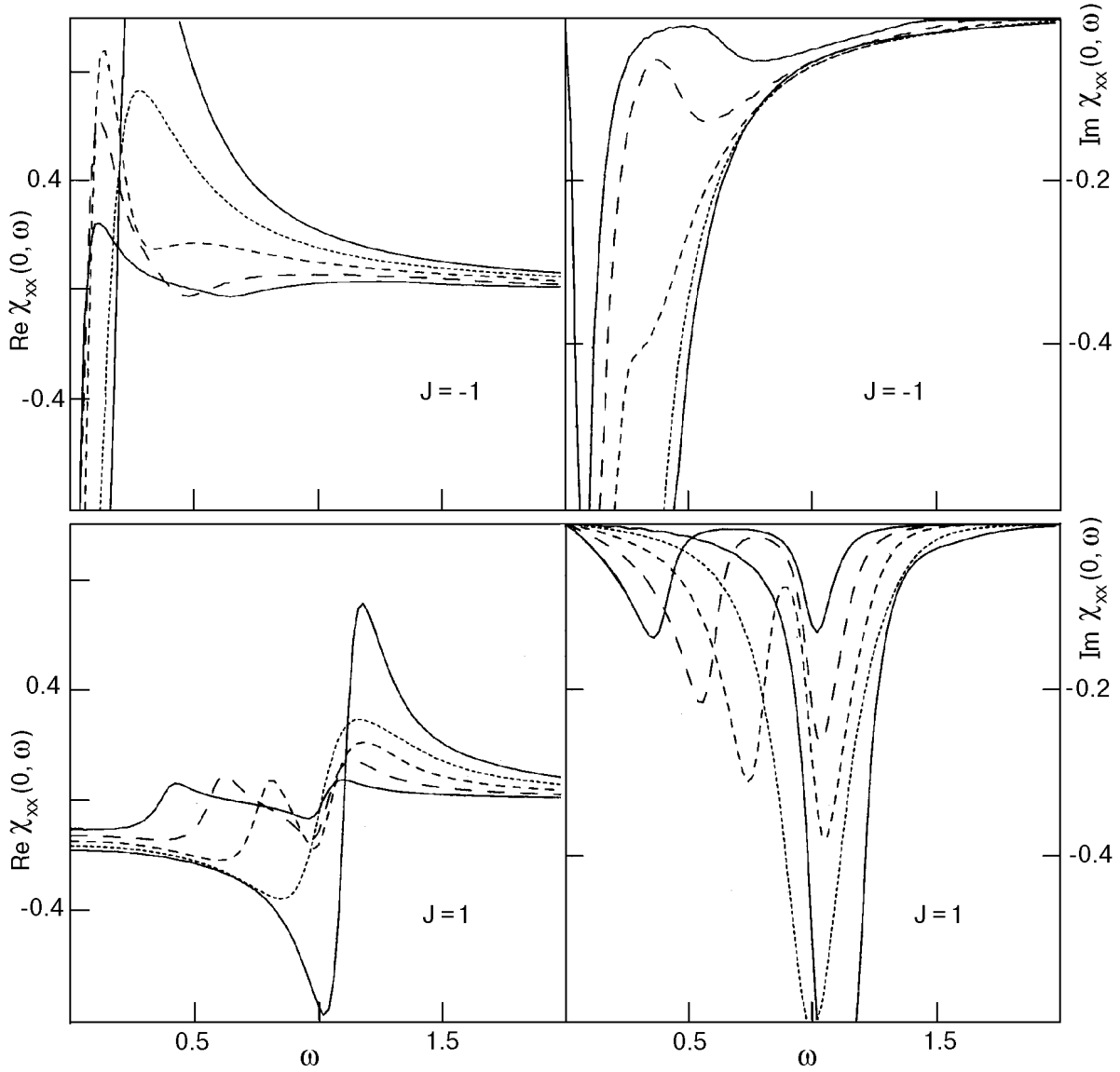

Fig. 2. $\chi_{xx}(0, \omega)$ versus ω for different values of transverse field at $\beta = 5$. The solid lines represent data for $\Omega = 0.2$ (these curves are also plotted in Fig. 1) and $\Omega = 0.6$; the long-dashed lines denote data for $\Omega = 0.3$; the short-dashed lines correspond to data for $\Omega = 0.4$; the dotted lines represent data for $\Omega = 0.5$.

their basis] pertain to infinite chains. The results of our numerical calculations were found to be in excellent agreement with the exact results obtained at $T = \infty$ (Ref. 6) and $T = 0$, $\Omega = J/2$ (Ref. 7) and with the notorious exact result for the *zz* correlation function [2]. It should be emphasized that the described approach allows one to study finite-size effects which, however, are beyond the scope of the present paper. Finally, we verified relations (2) which connect $\langle s_j^x(t) s_{j+n}^x \rangle$ with other correlation functions after these correlation functions are computed in a similar manner.

We shall discuss the dynamics of the transverse Ising model looking at the dynamic susceptibility

$$\chi_{xx}(\kappa, \omega) \equiv \sum_{n=1}^{N} e^{i\kappa n} \int_0^{\infty} dt\, e^{i(\omega + i\varepsilon)t} \frac{1}{i} \langle [s_j^x(t), s_{j+n}^x] \rangle \,, \quad \varepsilon \to +0 \,. \tag{9}$$

The frequency shapes of $\mathrm{Re}\, \chi_{xx}(0, \omega)$ and $\mathrm{Im}\, \chi_{xx}(0, \omega)$ at various transverse fields and temperatures are shown in Figs. 1 and 2. Small wiggles in the curves corresponding to $\beta = 5$ were introduced by the finite time cutoff in (9) because of rather slow decay of correlations versus time (especially for $\Omega = 0.2$, 1 and ferromagnetic intersite coupling). The wiggles can be removed either by

increasing the time cutoff in (9), which requires computer resources, or by increasing the value of ε, which slightly smooths the frequency shapes and decreases, in particular, the heights of their peculiarities. Usually, we set $\varepsilon = 0.001$–0.05.

Let us now turn to the discussion of the results. Figure 1 shows the dependence of Re $\chi_{xx}(0, \omega) - \omega$ and Im $\chi_{xx}(0, \omega) - \omega$ curves on Ω various temperatures. From these plots we easily see that Im $\chi_{xx}(0, \omega)$ exhibits two peaks for $\Omega = 0.2$ (the Ising-like case) and one peak for $\Omega = 1$ (the case of almost noninteracting spins in an external field). At low temperature $\beta = 5$ for $\Omega = 0.2$ Im $\chi_{xx}(0, \omega)$ reveals a high sharp peak in the vicinity of zero frequency $\omega \approx 0.03$ and a low broad peak at $\omega \approx$ ≈ 0.76 for ferromagnetic intersite coupling and two pronounced peaks at frequencies $\omega \approx 0.36$ and $\omega \approx 1.02$ for antiferromagnetic intersite coupling. In the case $\Omega = 1$ Im $\chi_{xx}(0, \omega)$ reveals one high and broad peak at $\omega \approx 0.51$ and $\omega \approx 1.50$ for ferro- and antiferromagnetic coupling, respectively . As the temperature is raised to $\beta = 1$, the situation qualitatively remains the same. For $\Omega = 0.2$ Im $\chi_{xx}(0, \omega)$ exhibits two lower and broader peaks compared with the preceding case, which are shifted to higher frequencies $\omega \approx 0.09$, $\omega \approx 0.94$ for ferromagnetic intersite interaction and to lower frequencies $\omega \approx$ ≈ 0.21, $\omega \approx 1.00$ for antiferromagnetic intersite interaction; in the latter case the low-frequency peak becomes higher than the high-frequency peak. For $\Omega = 1$ Im $\chi_{xx}(0, \omega)$ exhibits only one lower and broader peak compared with the case $\beta = 5$, which is shifted to higher frequency $\omega \approx 0.67$ for ferromagnetic coupling and to lower frequency $\omega \approx 1.42$ for antiferromagnetic coupling. At high temperature $\beta = 0.1$ the frequency profiles of Im $\chi_{xx}(0, \omega)$ almost coincide for ferromagnetic and antiferromagnetic couplings, although it is still possible to recognize two peaks for $\Omega = 0.2$ at $\omega \approx 0.13$, $\omega \approx$ ≈ 0.88 and $\omega \approx 0.15$, $\omega \approx 1.03$ for ferro- and antiferromagnetic coupling, respectively, and one peak for $\Omega = 1$ at $\omega \approx 1.00$ and $\omega \approx 1.10$ for ferro- and antiferromagnetic coupling, respectively.

In order to uderstand how two-peak shapes transform into one-peak shapes as the transverse field increases, we performed additional calculations of $\chi_{xx}(0, \omega)$ at $\beta = 5$ for $\Omega = 0.3$, 0.4, 0.5, 0.6 (shown in Fig. 2). As can be seen from Fig. 2, the high-frequency peak on the curve Im $\chi_{xx}(0, \omega) - \omega$ for $\beta = = 5$, $\Omega = 0.2$ at $\omega \approx 0.76$ for ferromagnetic coupling and the low-frequency peak at $\omega \approx 0.36$ for antiferromagnetic coupling with increasing transverse field move toward the low-frequency peak at $\omega \approx$ ≈ 0.03 for ferromagnetic coupling and toward high-frequency peak at $\omega \approx 1.02$ for antiferromagnetic coupling, which in turn become broader. The positions of the peaks are as follows: $\omega \approx 0.03$, $\omega \approx 0.57$ for $\Omega = 0.3$, $\omega \approx 0.05$, $\omega \approx 0.28$–0.36 for $\Omega = 0.4$ for ferromagnetic intersite interaction; $\omega \approx 0.56$, $\omega \approx$ ≈ 1.03 for $\Omega = 0.3$, $\omega \approx 0.75$, $\omega \approx 1.05$ for $\Omega = 0.4$ for antiferromagnetic intersite interaction. For $\Omega = 0.5$ two peaks have already coalesced: Im $\chi_{xx}(0, \omega)$ reveals one peak at $\omega \approx 0.10$ and $\omega \approx$ ≈ 1.00 for ferro- and antiferromagnetic coupling, respectively. Further increase of the transverse field leads to the shift of one peak to higher frequencies, i.e., $\omega \approx 0.15$ if $\Omega = 0.6$ and $\omega \approx 0.51$ if $\Omega = 1$ for ferromagnetic coupling and $\omega \approx 1.10$ if $\Omega = 0.6$ and $\omega \approx 1.50$ if $\Omega = 1$ for antiferromagnetic coupling.

In summary, we were able to numerically examine the dynamic properties of one-dimensional spin-$1/2$ Ising model in a transverse field and to evaluate the frequency-dependent susceptibility. These results seem to be important since, to the best of our knowledge, they constitute the only exact numerical results available. In addition, we hope that the main features of the susceptibility in the given limiting cases of small and large transverse fields would be observable in the measurements of dynamic dielectric constant of quasi-one-dimensional, hydrogen-bonded ferroelectrics materials like CsH_2PO_4 , $PbHPO_4$ (Ref. 12 and 13) ($\Omega < J/2$) and in the absorption spectrum measurements for J-aggregates [14,15] ($\Omega > J/2$). However, these problems and the reconsideration of some approximate approaches used earlier for analysis of experimental data require a separate study.

We wish to thank Professor L. L. Gonçalves and Professor J. Richter for stimulating discussions. O. D. is indebted to Mr. Joseph Kocowsky for continuous financial support.

1. E. Lieb, T. Schultz, and D. Mattis, *Ann. Phys.* **16**, 407 (1961).
2. Th. Nijemeijer, *Physica* **36**, 377 (1967).
3. P. Pfeuty, *Ann. Phys.* **57**, 79 (1970).
4. B. M. McCoy, E. Barouch, and D. B. Abraham, *Phys. Rev.* **A4**, 2331 (1971).
5. J. Lajzerowicz and P. Pfeuty, *Phys. Rev.* **B11**, 4560 (1975).
6. J. H. H. Perk, H. W. Capel, G. R. W. Quispel, and F. W. Nijhoff, *Physica* **A123**, 1 (1984).
7. G. Müller and R. E. Shrock, *Phys. Rev.* **B29**, 288 (1984).
8. A. R. Its, A. G. Izergin, V. E. Korepin, and N. A. Slavnov, *Phys. Rev. Lett.* **70**, 1704 (1993).
9. J. Stolze, A. Nöppert, and G. Müller, *Phys. Rev.* **B52**, 4319 (1995).

10. O. Derzhko and T. Krokhmalskii, *Ferroelectrics* **153**, 55 (1996).
11. O. Derzhko, T. Krokhmalskii, and T. Verkholyak, *JMMM* **157–158**, 421 (1996).
12. J. A. Plascak, A. S. T. Pires, and F. C. Sá Barreto, *Solid State Commun.* **44**, 787 (1982).
13. S. Watarai and T. Matsubara, *J. Phys. Soc. Jpn.* **53**, 3648 (1984).
14. J. Knoster, *J. Chem. Phys.* **99**, 8466 (1993).
15. H. Suzuura, T. Tokihiro, and Y. Ohta, *Phys. Rev.* **B49**, 4344 (1994).